To analysis of source mechanism of the 26 December 2004 Indian Ocean tsunami

L. I. Lobkovsky[1], R. Kh. Mazova[2], I. A. Garagash[3], L. Yu. Kataeva[2], and I. Nardin[2]

Received 5 September 2006; revised 18 September 2006; accepted 5 October 2006; published 29 October 2006.

[1] Tsunami in the Indian Ocean generated by a strong earthquake in Sumatra-Andaman region on 26 December 2004 led as known to catastrophic results at the coast of many countries of this region. In spite of intensive study of this event by a number of groups, the character of seafloor displacements in the source during this earthquake remains to be controversial. In this work, it is performed an analysis of physical aspects of similar earthquakes on the basis of keyboard model of tsunamigenic earthquakes. The numerical simulation of generation, propagation and run-up of surface water waves on the basis of simplified keyboard model of tsunamigenic earthquakes with vertical displacements of keyboard blocks in approximative geometry (without taking into account the real bathymetry) is also performed. It is obtained that tsunami waves generated by various combinations of keyboard block displacements are essentially different in character which fact leads to quite different picture of maximum run-up distribution along the near-field coast. It is performed the estimative computation for 26 December 2004 Sumatra-Andaman earthquake with taking into account of oblique character of the subduction zone characteristic for this earthquake. The computations performed explain the complex character of run-up distribution at nearest to the source coasts and are in a good agreement with run-up values at the Thailand coast. It is noted that such a model can account for more adequately the tsunami wavefield character in another regions of the Indian and the Pacific Ocean basins as well. *INDEX TERMS:* 3060 Marine Geology and Geophysics: Subduction zone processes; 3285 Mathematical Geophysics: Wave propagation; 4255 Oceanography: General: Numerical modeling; 7209 Seismology: Earthquake dynamics; *KEYWORDS:* tsunami generation, seismic source, wave propagation, subduction zones, keyboard-blocks.

Citation: Lobkovsky, L. I., R. Kh. Mazova, I. A. Garagash, L. Yu. Kataeva, and I. Nardin (2006), To analysis of source mechanism of the 26 December 2004 Indian Ocean tsunami, *Russ. J. Earth. Sci., 8,* ES5001, doi:10.2205/2006ES000208.

1. Introduction

[2] It is well known that 26 December 2004 and 28 March 2005 in the Indian Ocean there occurred two earthquakes: the first one, with magnitude 9.2, produced a largest tsunami which caused almost 300.000 deaths; and the second one, with magnitude 8.8, led to significant damages due to ground shaking but not produced a noticeable tsunami [for review, see, e.g., *Lay et al.,* 2005]. Both earthquakes occurred in the Indian Ocean west of the Sumatra Island and Thailand and they are related to the same part of Philippine and Sunda island arcs. Which cause is for so different results of earthquakes at so close earthquake magnitude? And though the cause of absence of strong tsunami due to 28 March, 2005 earthquake is not clear up to now, then it can be supposed that the difference is connected with features of seafloor displacements in the earthquake source.

[3] As known, the formation of tsunami depends on character and dynamics of displacements in earthquake source zone, i.e. on the initial seafloor displacements. As a rule, under computations of tsunami wave generation there are used the seismic data which indicate the rupture orientation in the source and the energy of tsunami. Then, the static hydrodynamical problem on the recount of seafloor displacement distribution to the ocean surface shape is considered. Further, the obtained displacements of the water surface with fixed length and height of the wave are taken as initial conditions and then it is performed the numerical

[1] P. P. Shirshov Institute of Oceanology, Russian Academy of Sciences, Moscow, Russia
[2] Nizhny Novgorod State Technical University, Nizhny Novgorod, Russia
[3] Institute of Physics of the Earth, Russian Academy of Sciences, Moscow, Russia

ISSN: 1681–1208 (online)

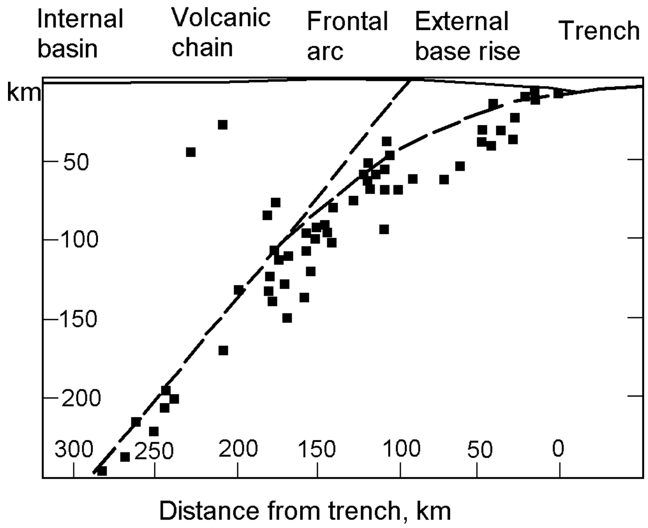

Figure 1. Sketch of subduction zone.

simulation of wave propagation in given basin with taking into account the real bathymetry. In present time, there are a number of numerical models and program complexes [see, e.g., *Goto et al.,* 1997; *Titov et al.,* 2005; etc.], which permits to perform accurately enough computations of tsunami wave propagation up to the coast. After the Indian Ocean tsunami the accuracy of such computations can be estimated by comparison of 3D-section in the Indian Ocean with satellite data on the water surface displacement at tsunami propagation [see, e.g., *Kulikov et al.,* 2005]. However, the question on the adequateness of the source model used at such simulations remains to be open. The features of tsunami generation, its parameters, initial velocity, characteristics of the coast (especially in the near-field zone) directly depend on the numerical model used to determine the initial movements of the seafloor in the earthquake source. Large uncertainty in these calculations stems from often poorly-defined seafloor displacements. Typically for the modeling purposes, the rupture orientation and associated displacement discontinuity is presupposed. Then, the distribution of the sea-bottom displacements is inferred from the static solution for a dislocation in the elastic half-space [*Okada,* 1992]. Such approach does not take into account the real structure of the Earth crust and lithosphere, and the initial stress-strain distribution in the zone of earthquake preparation [*Garagash and Ermakov,* 2001; *Garagash and Lobkovsky,* 2006]. In addition, the static solution does not allow to study the dynamic process of formation of sea-bottom displacements. The length of tsunami wave and its amplitude depend on all of the factors listed above. Development of an adequate numerical model to predict the sea-bottom movements at the moment of the earthquake will raise the accuracy of the situational modelling of a tsunami and its influence on the shore.

[4] In present time, it is elaborated a mechanism of strong earthquakes in subduction zones [*Lobkovsky,* 1988; *Lobkovsky et al.,* 2004]. It is known that narrow seismic belts of the Earth are connected with contact conditions on the boundaries of large lithosphere plates. Interaction of plates in subduction zone is responsible for seismic process in island arcs and active continental margins. The strongest earthquakes occur in subduction zones in the vicinity of gentle plane of a contact between the base of the island-arc wedge and roof of the underthrusting plate (Figure 1). The numerous geomorphological and geology-geophysical data demonstrates that island-arc wedge consists of separated large segments formed by transcurrent faults passing up to roof of the subducted plate (Figure 2).

[5] For example, traces of these faults are well seen in the bathymetric map of part of Philippine and Sunda island arcs where two strongest earthquakes under consideration occur (Figure 3). The presence of transcurrent faults requires to introduce new smaller interaction elements, so-called keyboard blocks of the frontal edge of the overriding plate. It was obtained that such minimal complication of conventional subduction scheme is quite enough to account for successfully the main features of seismic process in subduction zones [*Lobkovsky et al.,* 2004]. The characteristic size of keyboard blocks is about 100 km. Such "cutting into blocks" of frontal parts of island and continental margins determines structurally the size of strong earthquake source. Mainly, such sources are connected with keyboard blocks in the subduction zone which are deformed and "shooting" at stress release. But sometimes the source length corresponds to several adjoining blocks in which simultaneous release of accumulated elastic energy occurs. It can be proposed that in December 2004, in the Indian Ocean 8 or 10 keyboard blocks of the Sunda Island arc "shooted" almost simultaneously and this powerful "chord" produced a formation of huge source of earthquake and as a consequence appearance of giant tsunami.

[6] In this work, the simplified keyboard model with vertical displacements of blocks is analyzed. The long-term factors which determine the tectonic stress distribution in the Earth's core are the inhomogeneity of Earth's core me-

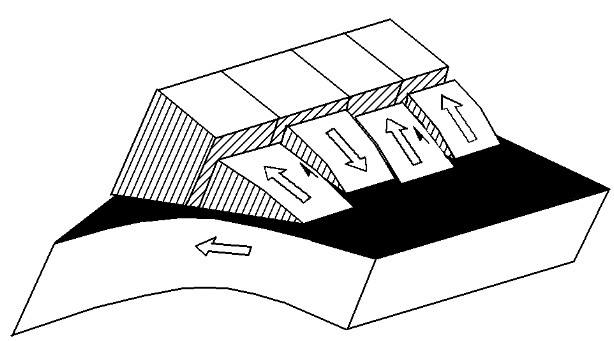

Figure 2. Keyboard model of the block structure in the frontal part of the island arc.

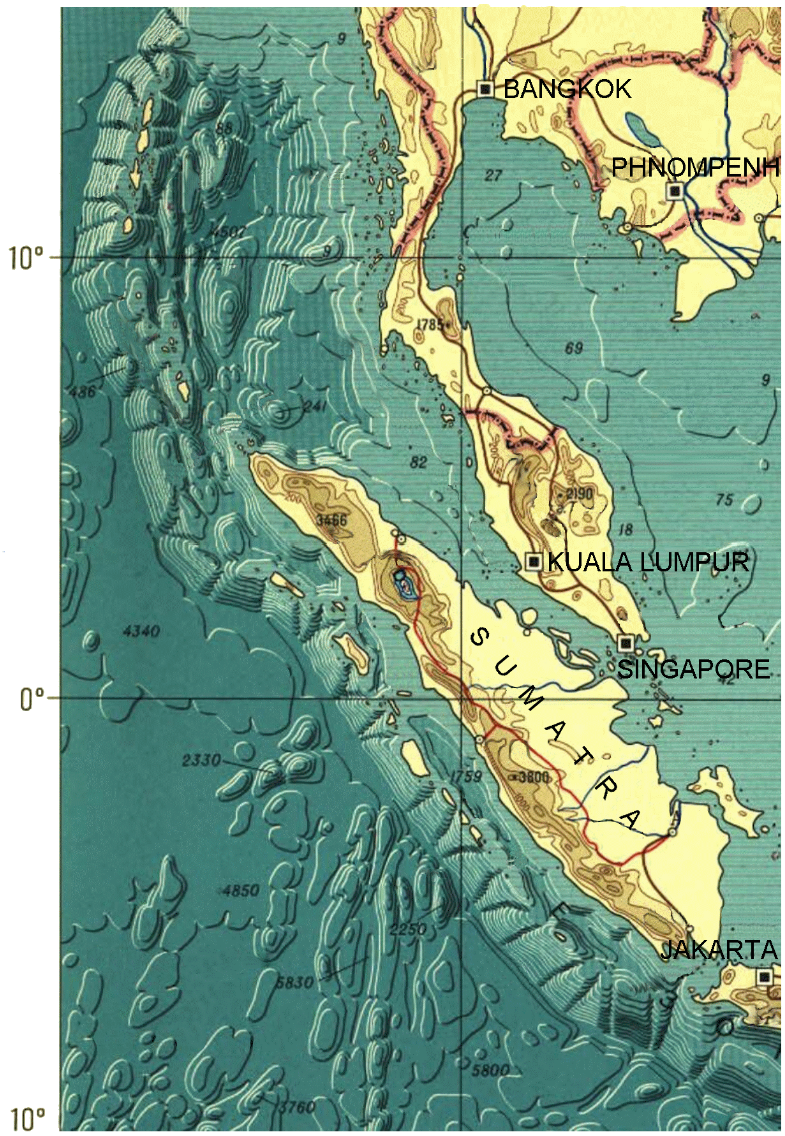

Figure 3. The bathymetric map of Philippine and Sunda arcs.

chanical properties and its density variations [*Lobkovsky et al.,* 2004]. At earthquake, initial stress distribution determines essentially the character of motion in the vicinity of the earthquake source. The earthquake occurs when stress at any region of contact surface overcomes the breaking point and the motion on it is accelerated. This process depending on earthquake preparation process and the initial stress level will proceed quite differently. And at the same vertical displacements the tsunami waves generated by them will be essentially different in character [*Lobkovsky et al.,* 2005a, 2005b, 2006]. In first part of this work (Sections 2–4) it is considered a formation of tsunami source without taking into account the initial tectonic stresses in the earthquake source. In second part of the work (Section 5) there is performed evaluation of affect of initial stress in zone of earthquake preparation.

2. Numerical Scheme to Model the Tsunami

2.1. Statement of the Problem

[7] The aim of this work is a numerical simulation of such a process in the tsunami source which would be a most relevant to possible motions occurring in the vicinity of earthquake source during the first minutes after starting of the earthquake. The process was modelled by vertical displacements of rectangular keyboard blocks with height B (Figure 4). The keyboard block size varied from 50 km to 150 km long and of 50 km wide. The number of keyboard blocks was varied from 3 to 8. In this work, the simplified keyboard

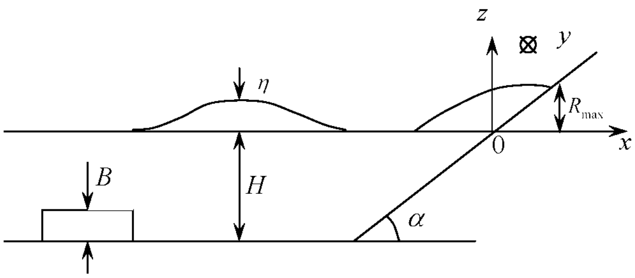

Figure 4. Geometry of generation and run-up of water wave at the sloping beach.

model with vertical displacements of keyboard blocks is analyzed, horizontal movements of keyboard blocks were not considered because of technical complexity to realize numerically the horizontal displacements of the order of 10 m for keyboard blocks, 50 km wide. It is considered a model problem of tsunami wave generation by dynamical source, its propagation and run-up on the sloping beach. The source is modelled by seafloor vertical displacements of keyboard blocks with given vertical velocity for each block. For the first set of computations, the source was located at the distance of 100 km from a beach being parallel to the coastline. The water height above the source was taken to be equal to $H = 1$ km. There was considered the wave propagation along even bottom in approximative geometry and run-up on a sloping beach (Figure 4).

2.2. Governing Equations

[8] To describe the process of wave generation and propagation in correspondence with above assumptions it was used the nonlinear system of shallow water equations (1),

$$\begin{cases} \dfrac{\partial \eta}{\partial t} + \dfrac{\partial}{\partial x}\big((H+\eta-B)\cdot u\big) + \dfrac{\partial}{\partial y}\big((H+\eta-B)\cdot v\big) = B_t \\ \dfrac{\partial u}{\partial t} + u\dfrac{\partial u}{\partial x} + v\dfrac{\partial u}{\partial y} + g\dfrac{\partial \eta}{\partial x} = 0 \\ \dfrac{\partial v}{\partial t} + u\dfrac{\partial v}{\partial x} + v\dfrac{\partial v}{\partial y} + g\dfrac{\partial \eta}{\partial x} = 0 \end{cases} \qquad (1)$$

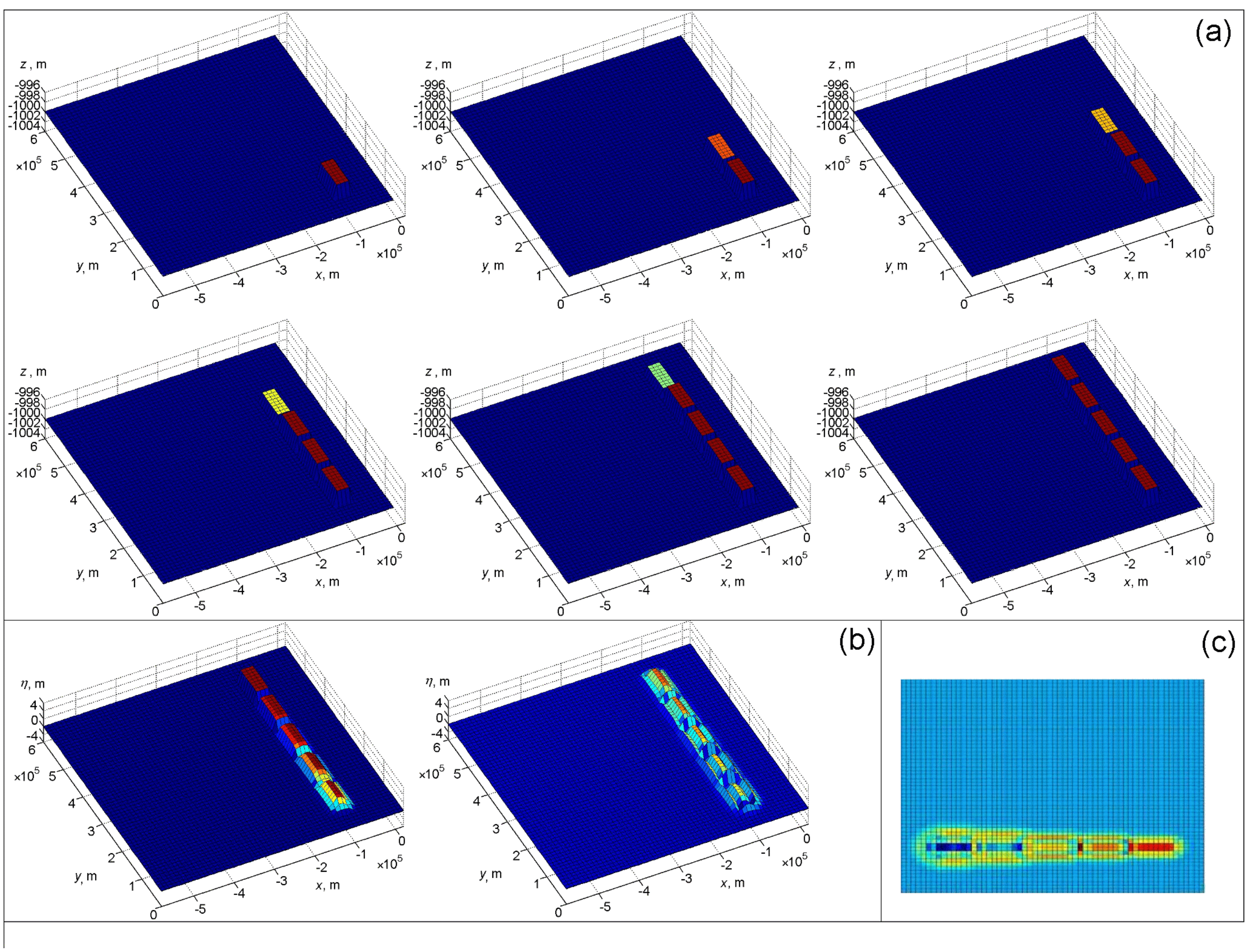

Figure 5. The example of successive block motion in earthquake source (a); The example of generation of surface water wave by seismic source: (b) for two time moments, (c) the view from upper point.

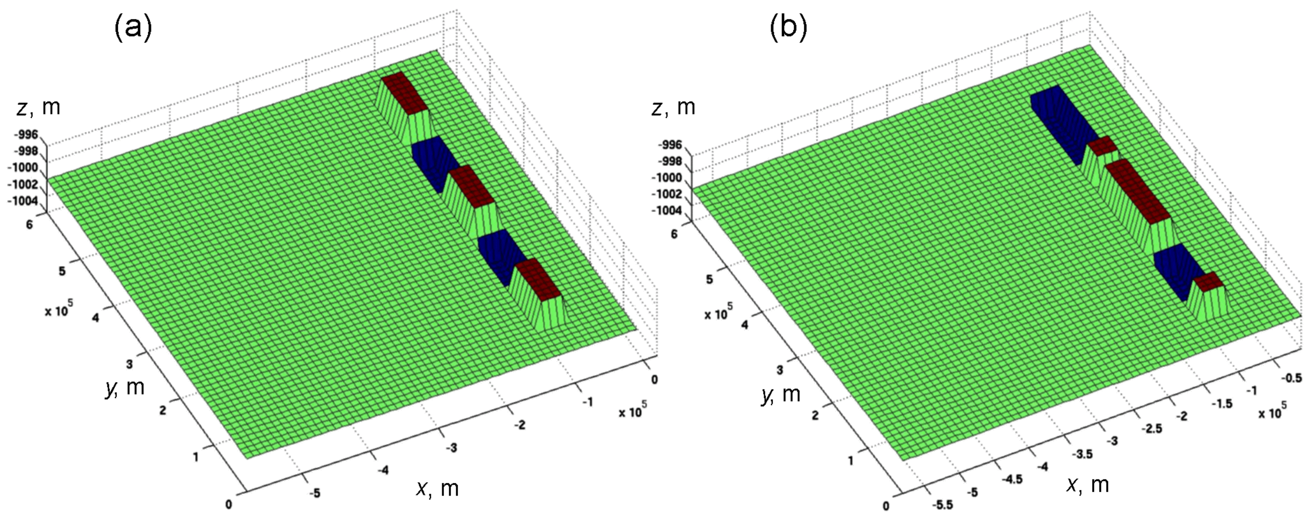

Figure 6. Successive motion of keyboard blocks in tsunamigenic earthquake source: the case of the same sizes blocks (a) and the case of blocks with different sizes (b).

where η is the surface elevation, u, v are the horizontal (x, y) particle velocity components of the wave motion, H is the undisturbed depth of the water, $B(t)$ is the seafloor deformation (seafloor displacement relative to initial position), g is the acceleration due to gravity [cf. with *Garagash et al.,* 2003]. The equations (1) were approximated by difference scheme according to [*Sielecki and Wurtele,* 1970]. It was used computation grid with space intervals $\Delta x, \Delta y$ and with time step Δt. The tsunami wavefield was computed on a Cartesian coordinate system. The size of the calculated region corresponds to 2400 km×2400 km. The size of computation grid was equal to 6.6 km. The computation was made every 10 s satisfying the Courant stability condition.

3. Numerical Simulation of Tsunami Generation, Propagation and Run-up: Keyboard Model of Source (Direct Subduction Zone)

[9] There was considered a dynamical source consisting of 5 rectangular keyboard blocks. In first set of computations keyboard blocks with the same size 100 km×50 km (Figure 5) were taken. In a second set of computations, lengths of corresponding five blocks were taken to be equal to 50, 100, 150, 50, and 150 km, respectively, and the width of all blocks was the same and equal to 50 km (Figure 6). Thus, source length for both sets of computations was equal to 500 km. The value of vertical displacement (upwards or downwards) of keyboard blocks from initial position, at water depth equal to 1000 m, was taken to be equal to 3 m for each keyboard block in both sets.

[10] The following scenarios were considered:

- uplift of first to fifth blocks, successively, one after another with the same velocities (0.05 m s^{-1} or 0.075 m s^{-1} or 0.15 m s^{-1});
- uplift of first to fifth blocks in various sequence but with the same velocities (0.05 m s^{-1} or 0.075 m s^{-1} and 0.15 m s^{-1});
- uplift of first to fifth blocks in various sequence but with different velocities;
- vertical displacement of blocks upward or downward in various sequence but with the same velocities (0.05 m s^{-1} or 0.075 m s^{-1} or 0.15 m s^{-1});
- uplift of first to fifth blocks but the motion of each next block begins before stopping of preceding one.

[11] Variations of these five scenarios are presented in Table 1.

[12] From Table 1 it is seen that value of run-up on a beach depends on the distance between the source and the coast (lines 2.2; 2.4; 2.5 in Table 1), on the velocity of block vertical motion in the source: slower motion, smaller run-up (lines 1.1; 1.2 in Table 1), and on the block size: at the same source (500 km long), its cutting to 5 blocks with lengths of 50, 100, 150, 50, and 150 km (with maximum size 150 km×100 km) leads to run-up increase from 3 m to 4 m (lines 1.2; 2.1 in Table 1), as compared with cutting of the same source to 5 equal blocks with size of each block 100 km×50 km (Figure 6). It is also seen that if the motion of the next block begins before stopping of preceding one then run-up value $R_{\max}$ increases to 20 percents, and run-down value $R_{\min}$ increases into 1.5 times (lines 1.1; 1.3 in Table 1).

3.1. Vertical Displacements of Keyboard Blocks in the Source Only Upwards

[13] The analysis of the results obtained permits to separate them on two characteristic features. To the first group

Table 1. Variations of Five Scenarios

no.	The behaviour of blocks	Displacement value of one block (m)	Motion time of one block (s)	Time of overall process (s)	$R_{\max}$ (m)	$R_{\min}$ (m)
1.1	Successive motion of blocks upward	3	20	120	3.8	2.5
1.2	Successive motion of blocks upward	3	60	180	3	2.1
1.3	Successive motion of blocks upward. Motion of next block begins before stopping of preceding one	3	20	120	4.6	3.6
1.4	Motion of blocks up from center in following sequence:					
	3 block,	3	40			
	2 block,	3	20			
	4 block,	3	60	200	3.9	2.6
	1 block,	3	20			
	5 block	3	60			
1.5	Motion of blocks up from center to edges of the source : 3, 4, 2, 5, 1.	3	20	120	4.0	2.5
1.6	Successive motion: 1, 3, 5 blocks upward, 2, 4 blocks downward	3	20	120	4.2	4.2
1.7	Successive motion up					
	3 block	3	40			
	2, 4 simultaneously	3	40	120	3.8	2.6
	1, 5 simultaneously	3	40			

no.	The behaviour of blocks	Displacement value of one block (m)	Motion time of one block (s)	Distance from the beach (km)	Time of the overall rupture process (s)	$R_{\max}$ (m)	$R_{\min}$ (m)
2.1	Successive motion of blocks upward	3	60	100	300	4.0	2.8
2.2	Successive motion of blocks; 2, 5 blocks downward	3	20	100	300	4	5.2
2.3	Successive motion of blocks; 1, 2, 5 blocks downward	3	20	100	100	4.3	5.5
2.4	Successive motion of blocks; 2, 5 blocks downward	3	20	50	100	5.5	4.3
2.5	Successive motion of blocks; 2, 5 blocks downward	3	20		100	7.5	4.0
2.6	Successive motion of blocks upward: 3, 4, 2, 5, 1	3	60	100	300	4.0	3.0

there are related events in which keyboard blocks in the earthquake source move only upwards (see, Table 1). As an example, let us consider events for lines 1.1 and 2.6. Figure 7 presents a space-time picture of behaviour of moving shoreline for 600 km part of the coast for these cases. There are well seen two wave fronts coming to a beach. The first front reaches the beach nearly after 25 min from the onset time of wave propagation from the source. And, at the same value

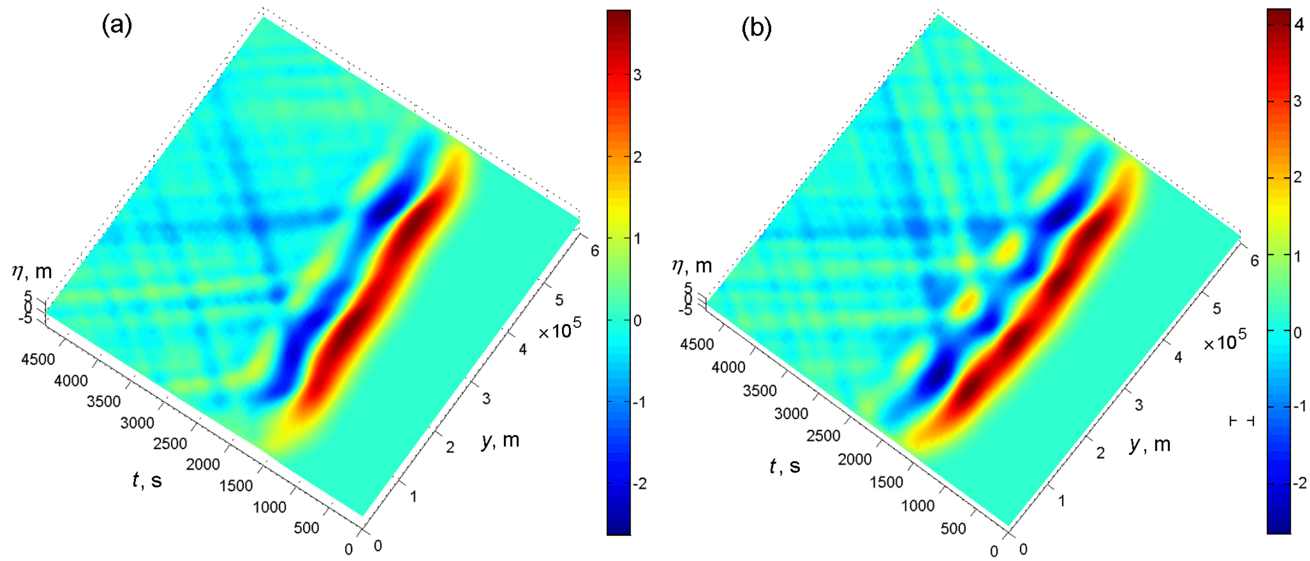

Figure 7. Space-time picture for the moving shoreline. y-axis is directed along the coast, height scale is in meters. (a) blocks of the same size, (b) blocks of different size.

of keyboard blocks (see Figure 5), first wave comes as continuous front and it reaches the beach near simultaneously almost in all points of the coast (Figure 7a). In the second case, the bend of the wave front is connected with different keyboard block size in the source and with sequence taken for the motion of blocks (Figure 7b). The second run-up wave front (Figure 7) is of more complex shape with alternation of crests and troughs along all the 500 km wave front. Such shape of front is formed depending on sequence of keyboard block motion in the source and on different velocity of their vertical motion.

[14] Figure 8 presents a distribution of maximum and minimum run-ups $R_{\max}$ at the coast for cases considered. It is well seen that for both cases maximum run-up $R_{\max}$ is about 4 m and maximum run-down from a beach $R_{\min}$ is near 2.8 meters. However, distribution of maximum run-up values along the coast is essentially different for each case considered. So, in the case of motion of the same keyboard blocks the maximum run-up is practically uniformly distributed along the coast with divergence of 10–17 percents (Figure 8a). Quite different situation arises for distribution of maximum run-ups in the case of upward motion of keyboard blocks with different sizes. The maximum run-up value distribution along the coast is between 0.5 m and 4 m (Figure 8b). The maximum values of water run-down from a beach $R_{\min}$ along the coast differ in 3.5 times.

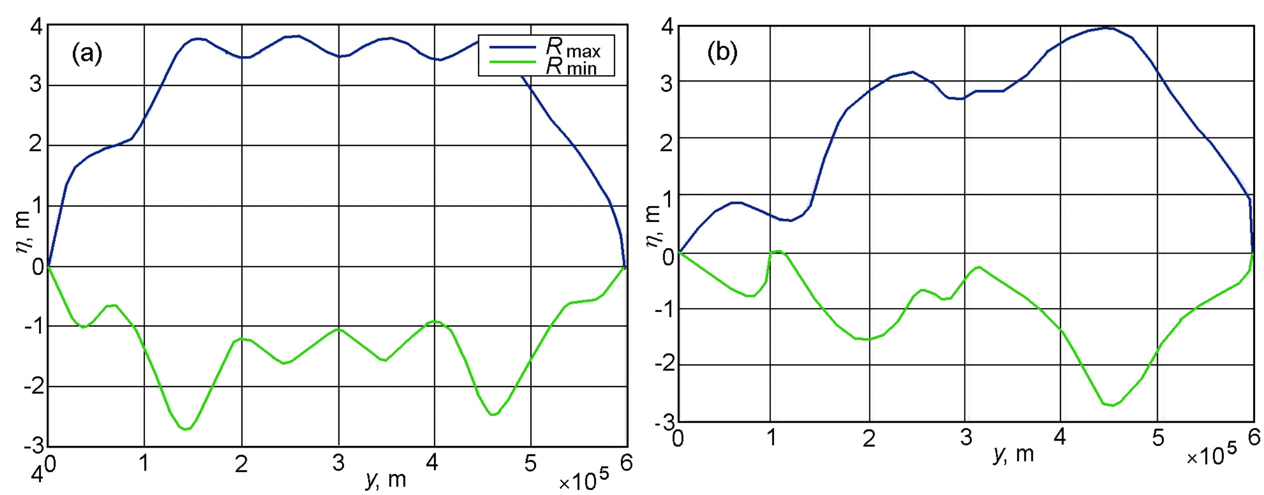

Figure 8. Distribution of maximum and minimum run-ups along 600 km part of the coast; y-axis is directed along the coast; $R_{\max}$ is a maximum run-up; $R_{\min}$ is a maximum run-down.

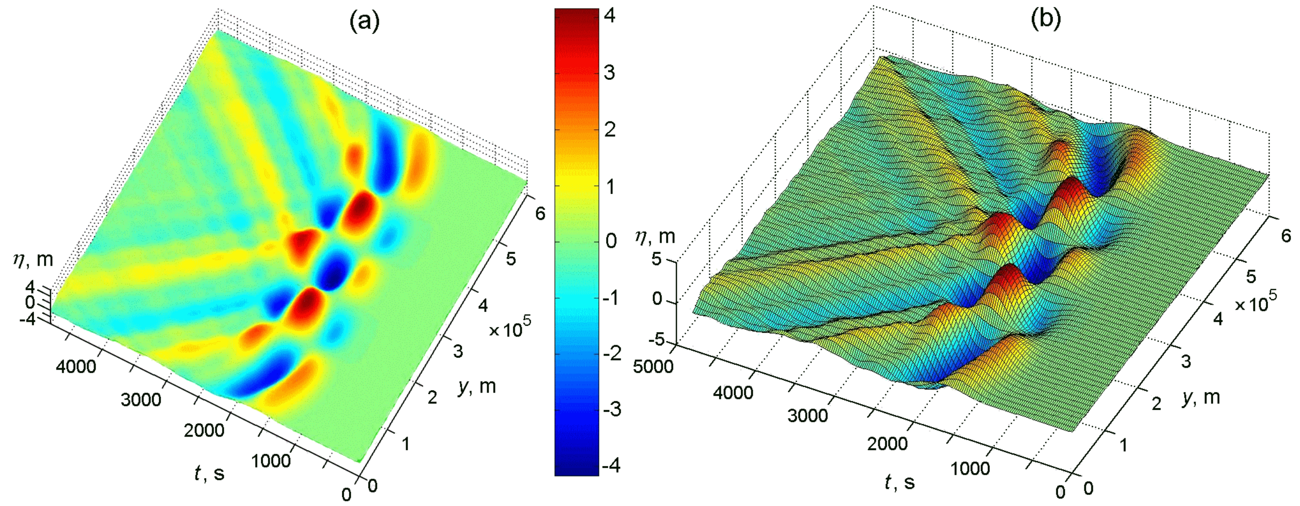

Figure 9. Space-time picture distribution of maximum wave run-up along shoreline for tsunami source consisting of keyboard blocks of the same size (Figure 6a); successive motion of blocks in the source: a) 2D simulation; b) 3D simulation.

3.2. Vertical Displacements of Keyboard Blocks in the Source Upwards and Downwards

[15] Quite another picture appears when there is presented the motion of keyboard blocks upward as well as downward. In Figure 9 it is presented an example of space-time picture for the case of vertical motion in the source of equal blocks, when 1, 3, 5 blocks are removed upward to 3 meters, and 2 and 4 blocks are displaced downward also to 3 meters (line 1.4 in Table 1). In this case, there appears a quite another picture of distribution of crests and troughs at the wave run-up on a beach. There are well seen three wave fronts. First of them is an insignificant run-down in ones points and a small run-up in another ones. The next wave front is alternation of maximum run-down $R_{\min}$ (vertical component) and run-ups $R_{\max}$ between -4 m and 4 m height. And third front with scattering of these values between -3 m and 3 m also is an alternation of crests and troughs. At analogous sequence of displacements but for keyboard blocks of different lengths it appears a very similar picture (Figure 10). Here, most values of run-up on the coast are for waves of the second front while most run-down is for waves of the first front. In the first place, it can be related to the waves generated by keyboard block downward motion since at various combinations of blocks in the source the depression wave can be followed by the elevation wave with larger height than that generated by motions of blocks only upwards [*Mazova and*

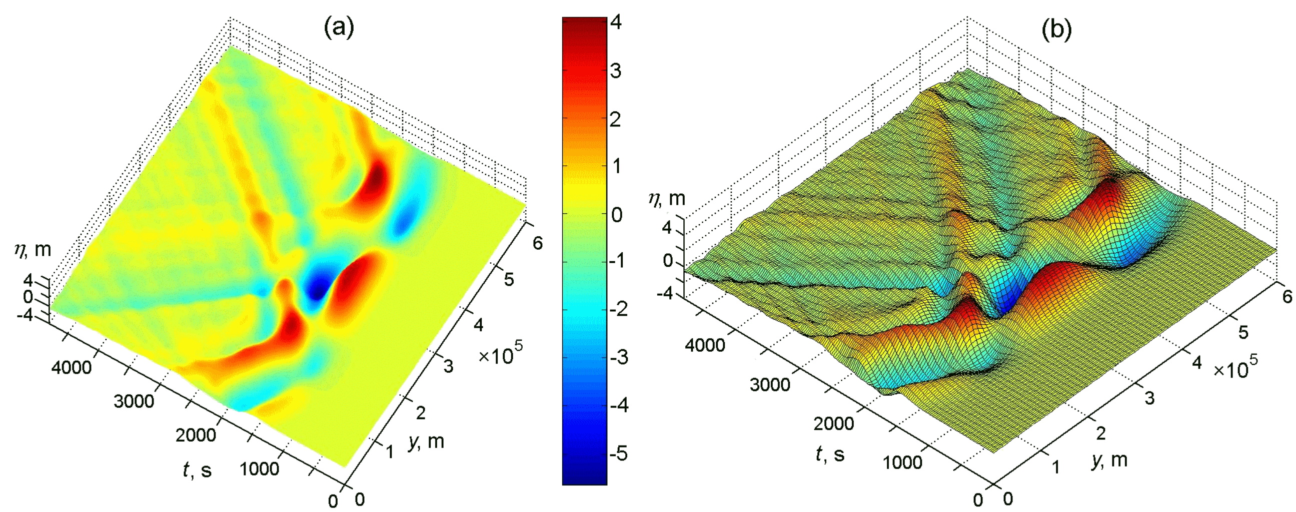

Figure 10. Space-time picture distribution of maximum wave run-up along shoreline for tsunami source consisting of keyboard blocks of the different size (Figure 6b); successive motion of blocks in the source: a) 2D simulation; b) 3D simulation.

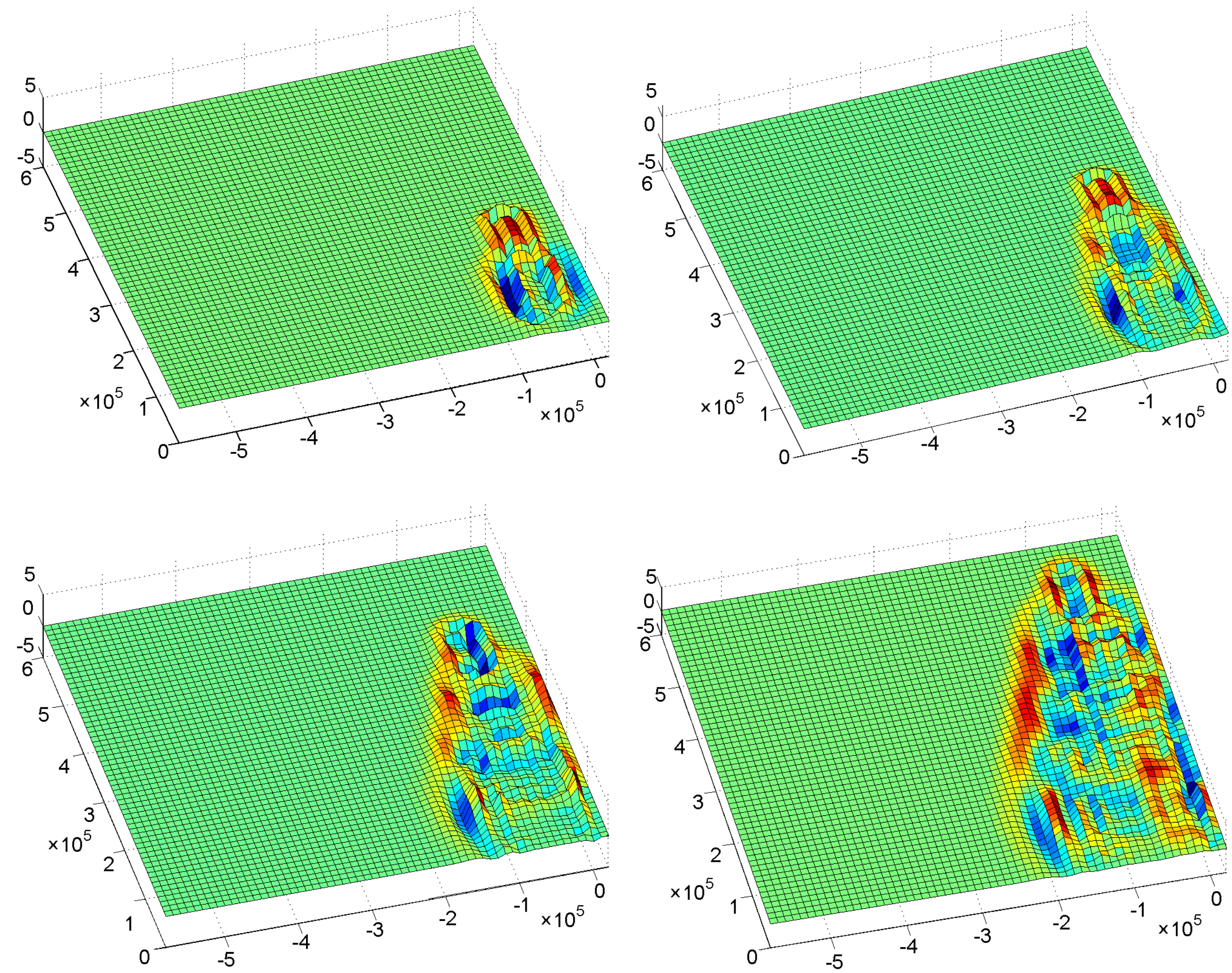

Figure 11. Propagation of surface water wave under rupturing in the source along the subduction zone.

Ramirez, 1999]. It is necessary to note that at rupture process in the source of tsunamigenic earthquake, surface water wave comes towards rupture spreading with velocity determined by that of vertical motion of keyboard blocks along the subduction zone. The wave generated by such source simultaneously comes along the subduction zone and propagates from source with different velocities.

[16] In Figure 11 it is presented the propagation of surface water wave along the source at rupturing in the source during the earthquake.

[17] The analysis performed demonstrates that at motion of keyboard blocks in the earthquake source the sequence of their displacements, the change of the keyboard block size in 1.5–2 times, and the change of rise velocity in two times provides only insignificant change of the run-up value. However, the distribution of maximum run-ups and maximum run-downs along the coast is essentially different, this difference can be of up to 8–10 times.

4. Numerical Simulation of Tsunami Generation, Propagation and Run-up: Keyboard Model of the Source (Oblique (Sumatra-Andaman-Like) Subduction Zone)

[18] The above performed study was then applied under analysis of tsunami wave generation due to the 26 December 2004 Indian Ocean earthquake. The earthquake source was located west of Sumatra Island northward along the oceanic subduction zone. The extent of the source was estimated near 1000 km [see, e.g. *Lay et al.,* 2005].

[19] In this work, there are considered two possible scenarios of seafloor motions in the earthquake source (subduction zone) for geometry close to that of oblique subduction zone (Figure 3) in the source of Sumatra-Andaman earthquake [cf. with *Lobkovsky et al.,* 1991]. These motions were ap-

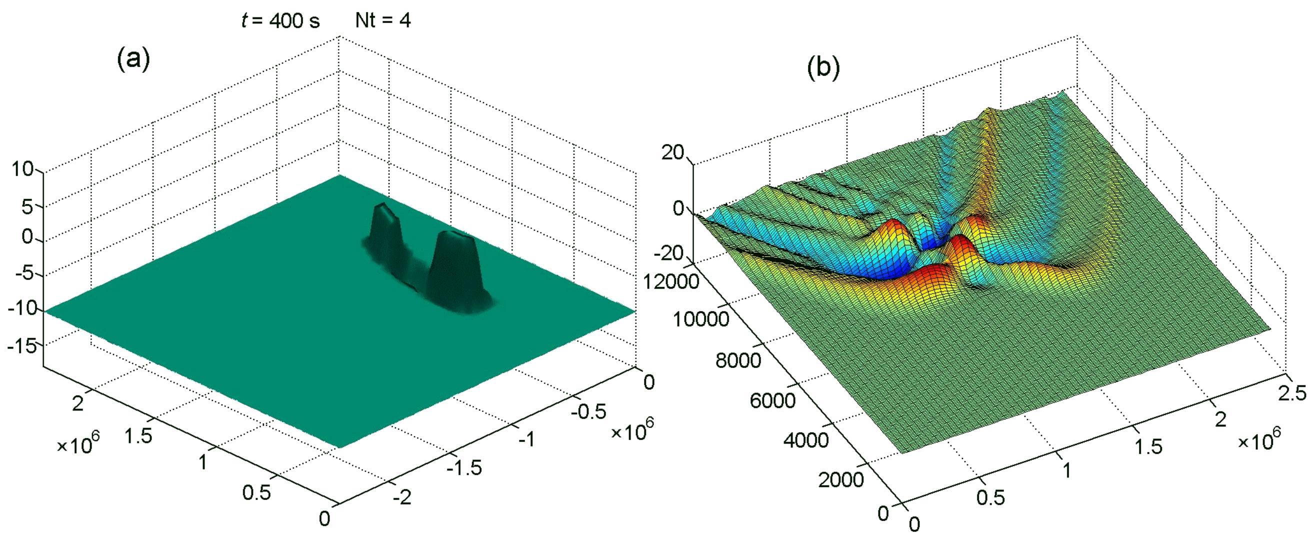

Figure 12. Modelling of the source of tsunamigenic earthquake 26 December 2004 by motion of three keyboard blocks rising along the subduction zone one after another from south to the north (a); space-time picture of the moving shoreline(b). Maximum run-up is equal to $R_{\max} = 9.5$ m, run-down $R_{\min} = 7.5$ m.

proximated by motion of several keyboard blocks with different size. The location of the source relative to the Sumatra Island and Thailand beaches, the ocean depth in the source zone, extent of the near-coast zone (slope length and shelf slope angle), as well as possible parameters of the earthquake process were taken into account at given simulation. It was considered a run-up on a plane slope. However, modelness of the problem is that it was not taken into account the real bathymetry of the ocean and estimations were made for wave propagation on the even bottom. Such approach corresponds to small-scale tsunamizonation when ocean bottom relief can be considered as smoothed one [*Soloviev et al.,* 1977]. It was mainly considered run-up at the nearest to the earthquake source beach corresponding to the Thailand coast.

4.1. Source Consisting of Three Keyboard Blocks

[20] The location of the first keyboard block with size 400 km×150 km corresponds to the region of northwest of Sumatra Island where the first strongest quake occurs. Second keyboard block 300 km long is of width decreasing from 150 km to 100 km northward. Third keyboard block is also of 300 km long, and the width is decreased from 100 km to 50 km. The keyboard blocks moves successively: first shifts upward to 9 meters, second shifts downward to 3 meters, third shifts upward to 5 meters. The entire time of block motion is equal to 330 s. Figure 12 shows the location of keyboard blocks (a) and space-time picture of the moving shoreline (b). Animation 1 (see online version) shows dynamics of wave generation, propagation, and run-up on the beach. It is well seen that to a beach it comes a wave train: two large waves which are followed by a strong sea recession. Then, in addition, three waves are followed them. First front comes in nearly 1.5 hours after the beginning of the motions in the source. Its height is not very large, up to 3 meters. Then, 20 min later, it comes the wave with height 9.5 meters. It is followed by alternating wave run-ups and run-downs with somewhat smaller height (depth).

4.2. Source Consisting of Eight Keyboard Blocks

[21] The location of the first keyboard block also corresponds to northwest Sumatra Island and is 300 km long while all another blocks are 100 km long and 150 km wide. The keyboard blocks moves successively in the following order:

Block	Block length, km	Vertical shift	Shift value, m	Motion time, s
1	300 km	upward	7	60
2	100 km	upward	3	40
3	100 km	downward	3	60
4	100 km	upward	4	50
5	100 km	upward	2	30
6	100 km	downward	2	60
7	100 km	upward	3	40
8	100 km	upward	2	60

Figure 13 shows the location of keyboard blocks (a) and space-time picture of moving shoreline (b). Animation 2 (see online version) shows dynamics of wave generation with scale of maximum run-up on the beach and 9 fragments of surface water wave generation. It is well seen that given parameters of keyboard blocks in the earthquake source lead to one significant wave run-up on the beach and essential run-down and then to several more weak waves. Maximum run-up in this case is equal to 11 meters.

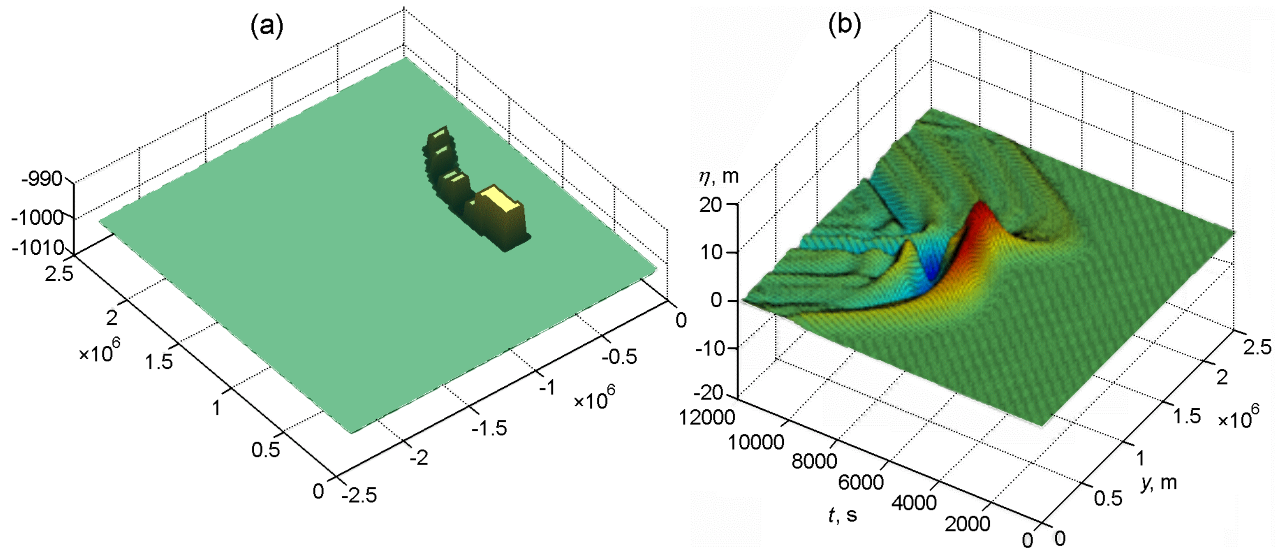

Figure 13. Modelling of the source of tsunamigenic earthquake 26 December, 2004 by motion of eight keyboard blocks moving along the subduction zone one after another from south to north (a); space-time picture of the moving shoreline(b). Maximum run-up is equal to $R_{\max} = 11$ m, run-down $R_{\min} = 10$ m.

[22] The further performed numerical simulation of the surface water wave generation by motions of keyboard blocks in the source of given earthquake demonstrates that under keyboard block motion in the source from south to north, along the subduction zone, the keyboard block sizes and velocity with which they move upward (downward), as well as velocity with which this motion comes along the subduction zone are the essential factors.

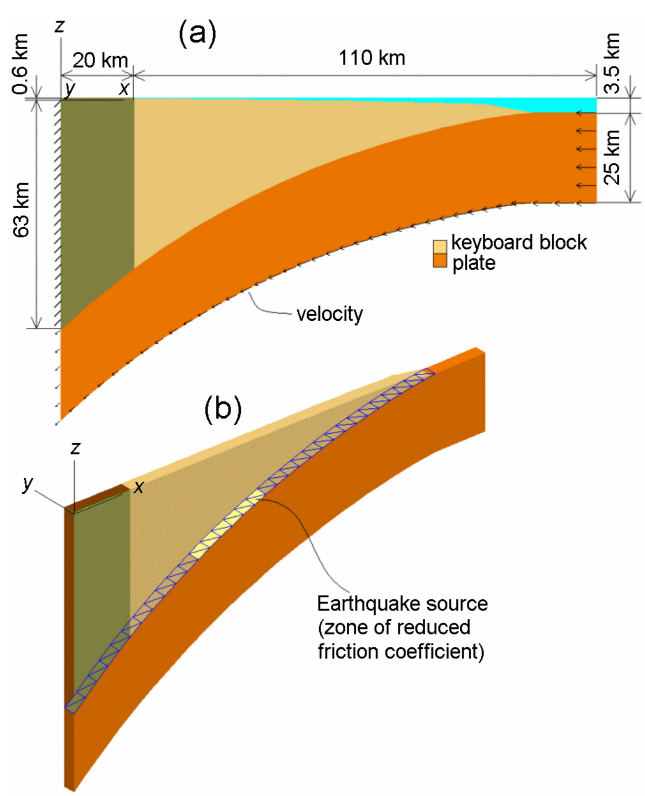

Figure 14. Sketch of the computational model subduction zone.

5. Influence of Initial Stress Distribution in Zone of Earthquake Preparation to Tsunami Formation

5.1. Analysis of Initial Stress Distribution in Seismic Source

[23] The distribution of initial stresses can affect the character of the motion in the vicinity of a seismic source. It can be demonstrated by the example of the plain-strain problem for the keyboard model (Figure 2). The material of keyboard block as well as moving and frontal plates is considered to be an elastoplastic medium with given parameters and satisfying the Mohr-Coulomb yield criterion. The velocity distribution in the bottom of the moving plate (Figure 14a) is dictated by the slow mantle motion. This velocity is causing the accumulation of elastic stresses in the system. On the contact of the plate and keyboard block the dry friction force acts. An earthquake occurs when stresses on a local area of the contact surface exceed the strength limit and resulting slip (Figure 14b) is accelerating. Since the dynamic interface friction is less than the static friction, the dynamic frictional resistance falls sharply and the earthquake occurs. This process depends on the interseismic time and the level of the initial stresses which were achieved before the nucleation of the seismic motion and can be highly variable. In the case

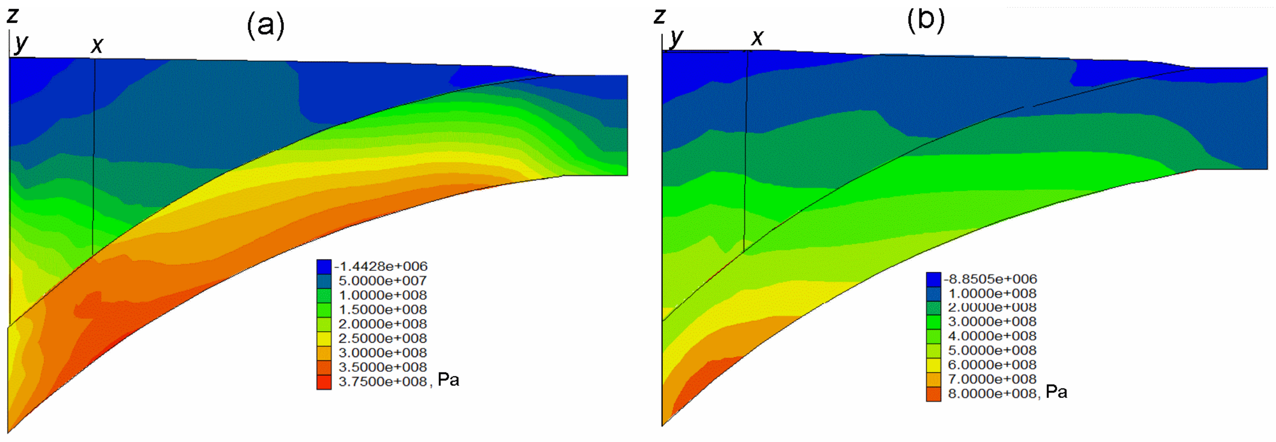

Figure 15. Distribution of the maximum shear stress for small (a) and large (b) time of elastic energy accumulation.

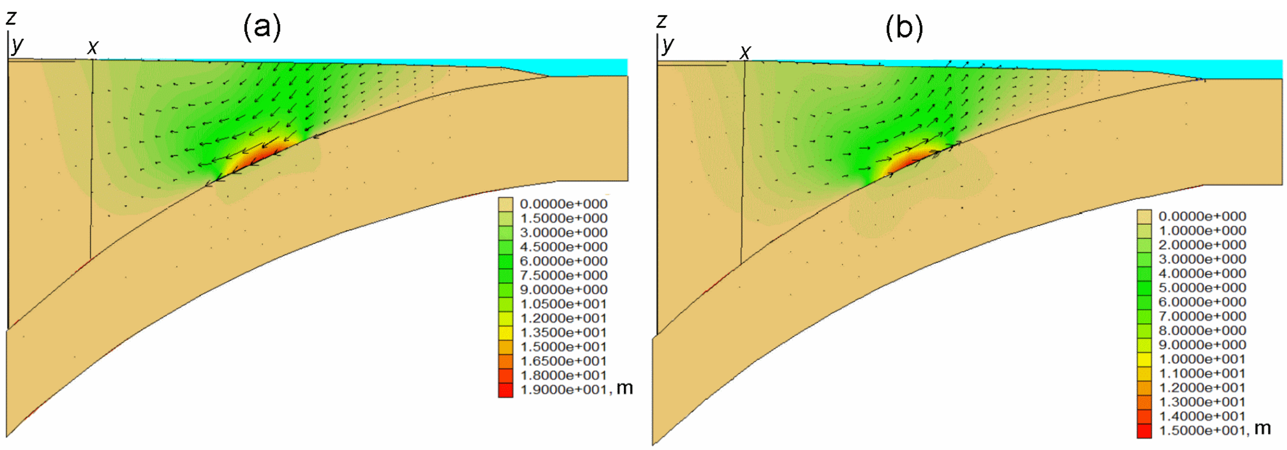

Figure 16. Distribution of residual displacements for the short (a) and long (b) time of elastic energy accumulation.

of small time of preparation, relatively small shear stresses (Figure 15a), residual friction angle value (e.g. of 8.3°), the displacements in the earthquake source (Figure 16a) will be oriented in the direction of the plate movement. Otherwise, in the case of large time of preparation and the greater level of initial shear stresses (Figure 15b), the displacements will be oriented in the opposite direction (Figure 16b). Though the maximum vertical displacement of the sea bottom in

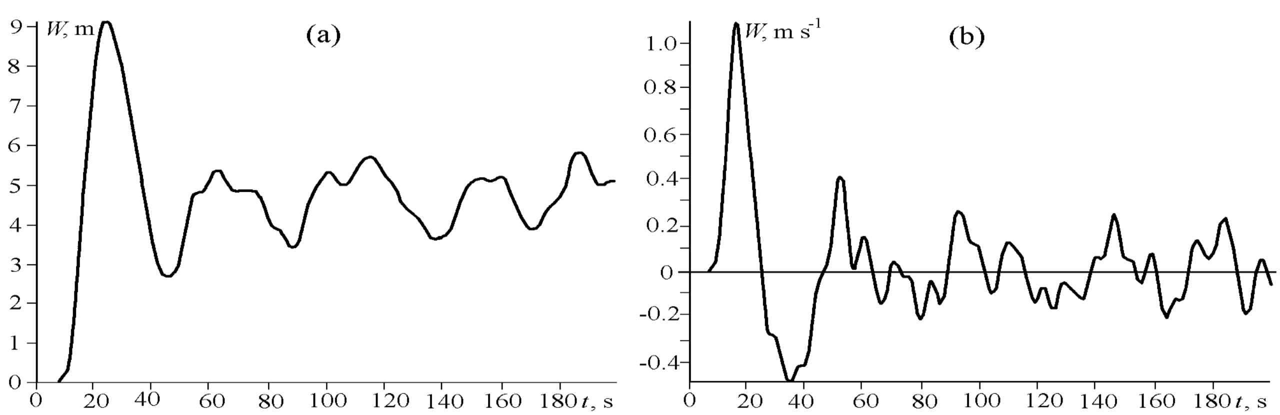

Figure 17. Time plots of vertical displacement (a) and vertical velocity (b) of sea bottom during the earthquake.

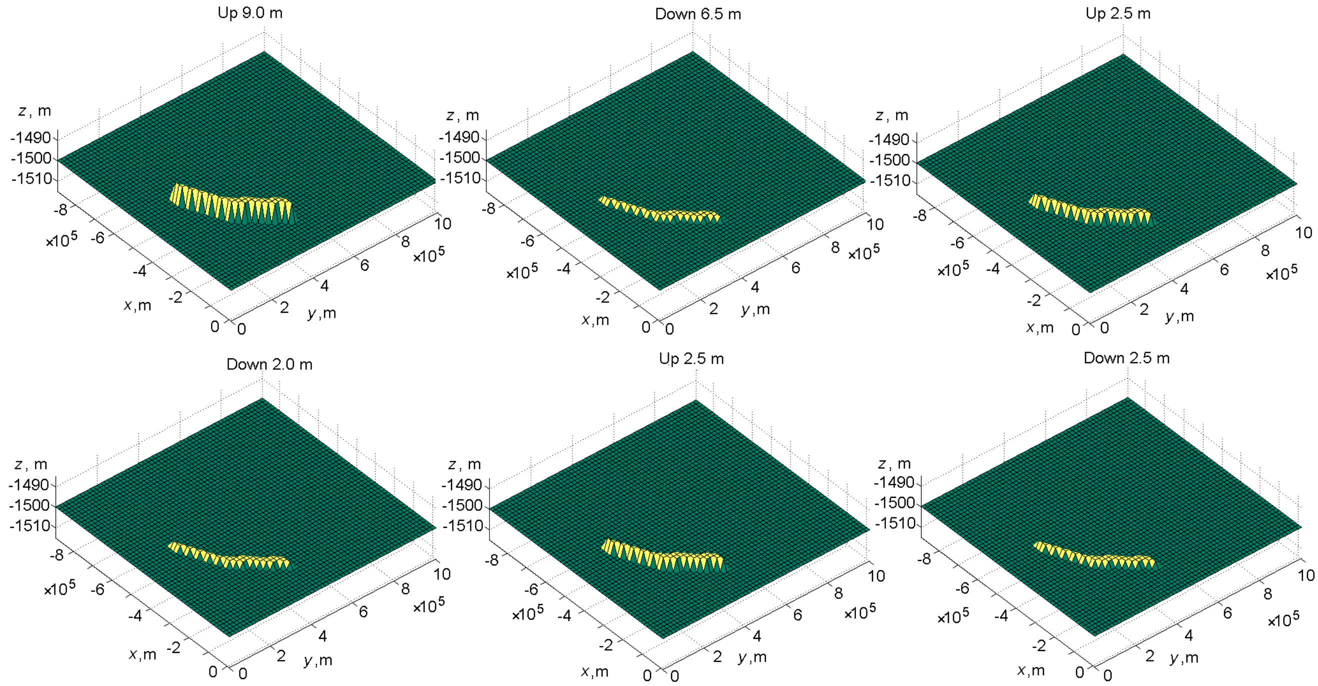

Figure 18. Illustration of dynamical model of seismic source with keyboard blocks. See also Animation 3 in online version.

both cases makes about 5 meters generated tsunami waves will be very different. In Figure 16 there are presented residual keyboard block displacements. However, the analysis of dynamics of the transient displacement of a sea bottom shows that the dynamic component of the vertical displacement can exceed the residual displacement of the bottom established after the earthquake by the factor of two. In Figure 17a there are shown the variation of the vertical displacement of the bottom at the point A (Figure 14b) during an earthquake from its nucleation to. Corresponding plot of the bottom velocity is shown in Figure 17b. It is obvious that the proper specialization of magnitude and temporal variation of displacements and velocities of the sea bottom during an earthquake are critical in the problem of tsunami wave formation.

5.2. Numerical Simulation of Tsunami Wave Generation, Propagation and Run-up with Taking into Account the Dynamics in the Earthquake Source

[24] The results of numerical simulation of tsunami wave generation performed under sea bottom displacements corresponding to Figure 17a are presented in Figure 18 and Animation 3 (see online version). We have considered a hypothetical (model) source which can be attributed to Sumatra segment of 2004 earthquake source. The source size was taken equal to 400 km×150 km. It was considered a movement of seismic source as a whole according to Figure 17.

[25] Since it is considered local problem then temporal picture of wave coming to shoreline will reflect the process of surface water wave formation in seismic source. It is well seen that if period of bottom oscillations is of the order of 30–40 s (i.e. time of uplift and subsidence of keyboard block is of the order of 20 s) then such movements can be considered as instant bottom displacements. Then, because of incompressibility of liquid and hydrostatic pressure the tsunami source is formed as in the piston model, and the wave height above seismic source will be that as value of displacement in the source. Second uplift of bottom after 35–40 s gives no possibility for the first front to be formed clearly. As result, there occurs superposition of two fronts and depending on the source the wave height will be between 1 m and 2.5 m. Mostly it is a first wave.

[26] Further shake on the bottom leads to appearance of large trough at the water surface, near 4 m in amplitude. In the Figure 19a it is seen two to three well expressed wave fronts while in seismic source the process is continued during five periods (see Figure 17).

[27] The Figure 19a corresponds to process of instant release of elastic stress at the rupture surface. It occurs as result of sharp decrease of the friction angle (from 20° to

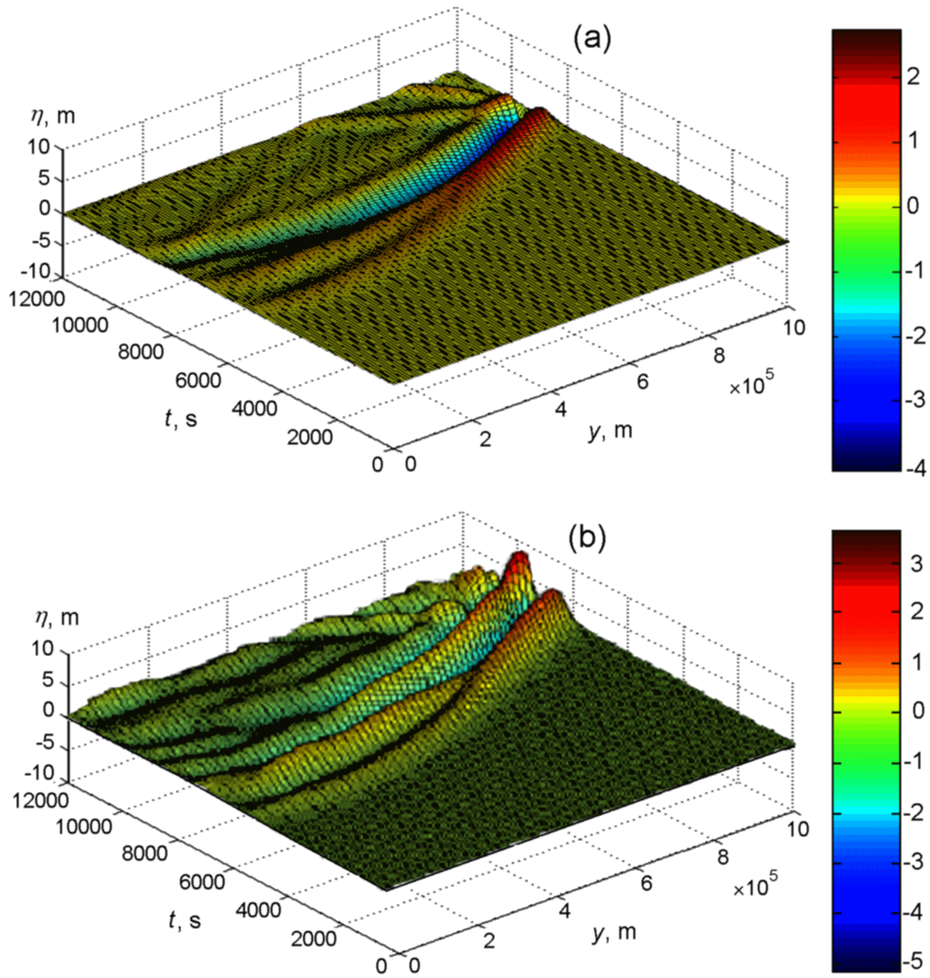

Figure 19. Space-time picture of wave distribution at the coming to a beach.

8.2° for given case). If it takes place a transient process and friction angle is a function of time $f(t)$ then the effect of this to character of surface displacements will be changed. The jump is a "rigid reaction", in prolongated $f(t)$ process the period of sea bottom oscillations will be larger. The increase of oscillation period in three to five times essentially changes the character of formation of surface water wave by seismic source.

[28] The space-time picture of behaviour of the wave at the shoreline for given case (Figure 19b) is essentially distinct from the case with "rigid reaction" (Figure 19a). In this figure, there are more clearly looked all wave fronts and it is well seen that as a most is a third wave. In Figure 20 it is well seen clearly expressed fronts of all waves. Figure 21 presents a distribution of values of run-up at the beach and run-down from the beach for moments of maximum run-up ($R_{\max} =$ 4.5 m) and $R_{\min}$ is more than 5 m in magnitude. Using computation method above proposed it was computed a number of scenarios of generation and propagation of tsunami wave in Indian Ocean basin for tsunami 26 December 2004. In Figure 22 it is presented one of version of computations at which it was considered a seismic source 1400 km long and 150 km width consisting of 14 blocks with equal length

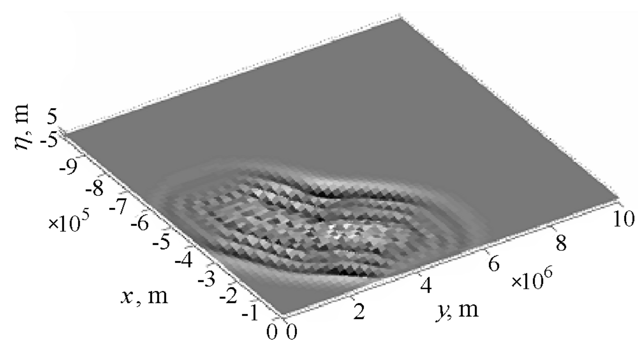

Figure 20. Generation of surface water wave by seismic source.

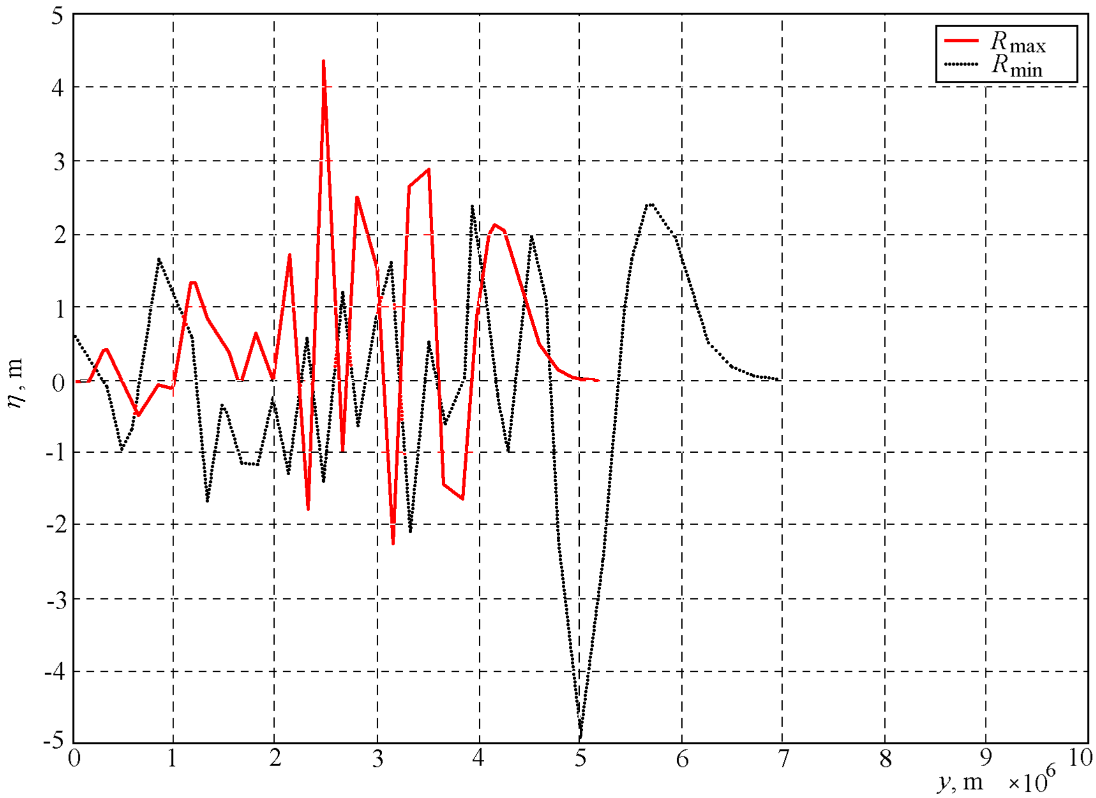

Figure 21. Distribution of values of run-up at the beach and run-down from the beach for moments of maximum run-up $R_{\max}$ and run-down $R_{\min}$.

[*Hirata et al.,* 2006. Three time moments of generation in tsunami source are presented in the figure: $t = 20$ s; $t = 2$ min 20 s; $t = 4$ min 50 s, at which it was taken into account the initial stress distribution in seismic source for each block, the moments when tsunami attacks the Sumatra island are: $t = 16$ min 30 s; $t = 33$ min 10 s; the moment when tsunami attacks the Thailand is: $t = 1$ h 50 min; further propagation of tsunami to Indian coast and attack to east coast of Sri Lanka at $t = 2$ h 30 min.

[29] Thus, analysis of the scenarios of generation of tsunami wave with using of elastoplastic model of subduction zone permits to explain unexpected nonuniform distribution of tsunami waves for both near-field and far-field coasts.

6. Conclusion

[30] The numerical simulation of dynamical process in the earthquake source performed in this work on the basis of keyboard model demonstrates that tsunami waves generated by different combination of keyboard block motions have an essentially different character what leads to different picture of distribution of maximum run-ups along the coast. Taking into account of oblique character of the subduction zone characteristic for 26 December 2004 Sumatra-Andaman earthquake gives a good agreement with run-up values observed at the Thailand coast. It is noted that such a model can more adequately account for the character of the wavefield in other regions of the Indian and the Pacific oceans also.

Electronic Supplement

[31] The online version of this paper includes four animations showing processes of generation, propagation and run-up of tsunami waves on the beach. Animations 1 and 2 show tsunami waves generation for the simplified model of seismic source, which consists of three and eight blocks correspondingly, propagation of tsunami waves and running-up them on the beach. Sizes and locations of blocks correspond to the seismic source, caused the catastrophic tsunami of 26 December 2004 in the Indian Ocean. Successive motion of blocks with different velocities was set (see text for more detail).

[32] Animation 3 shows movements of blocks in the seismic

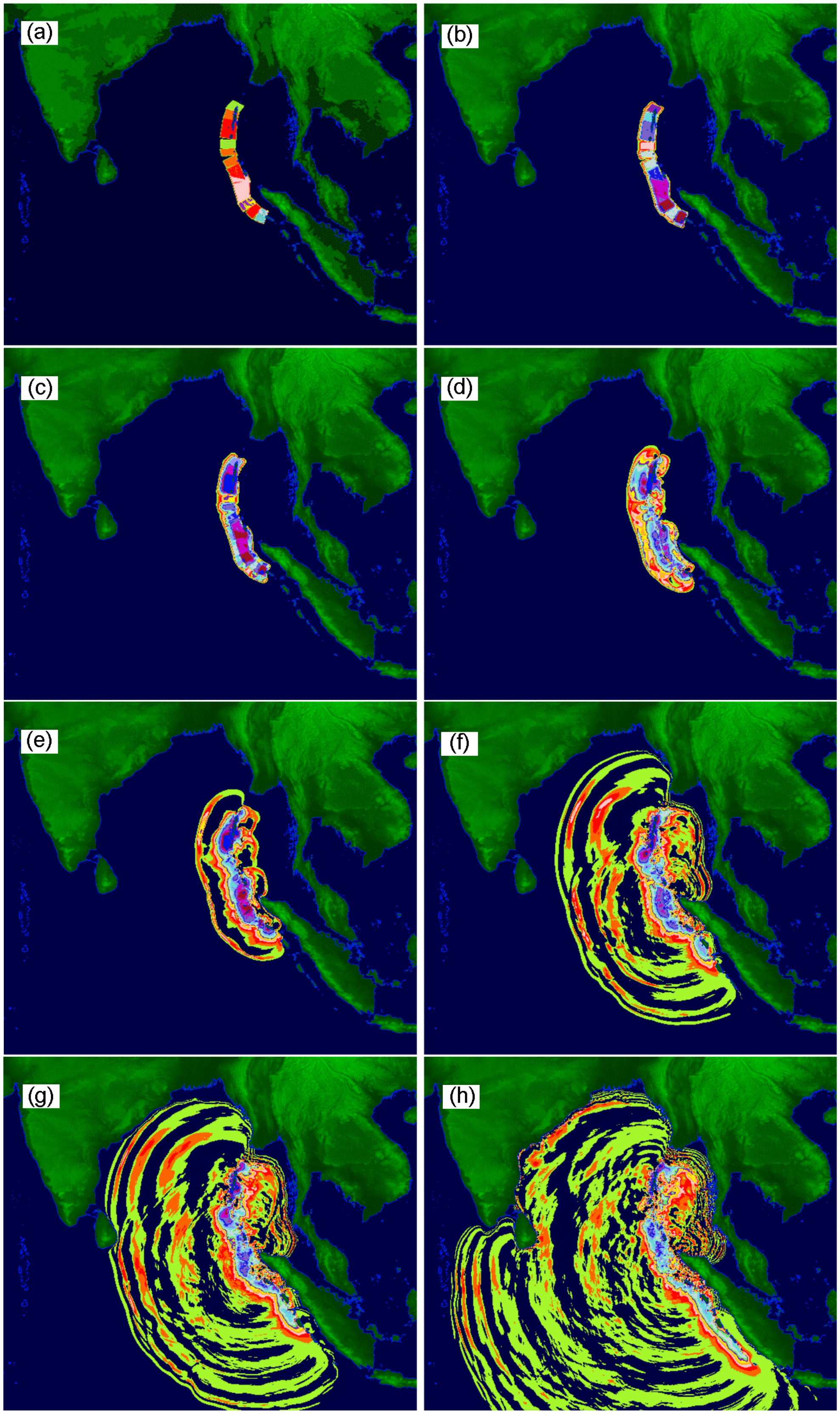

Figure 22. Generation and propagation of tsunami waves in the basin of the Indian Ocean for the seismic source comprising 14 blocks for the time moments: a – t=20", b – t=2'20', c – t=4'50", d – t=16'30", e – t=33'10", f – t=1h50', g – t=2h30', h – t=4h18'.

source during the earthquakes. Calculations were made for the stressed state of blocks at the earthquakes preparatory stage. (see text for more detais).

[33] Animation 4 for the tsunami in the Indian Ocean of 26 December 2004 is based on the results of numerical simulation of surface waves generation for the seismic source consisting of 14 blocks (see [*Hirata et al.,* 2006]). Movements of blocks in the seismic source were calculated for the stressed state of blocks, the propagation tsunami waves from seismic source was calculated up to 10-m isobath.

References

Garagash, I. A., and V. A. Ermakov (2001), Use of geological and geophysical models for simulating of crust stress state on the example of Sakhalin and Tien-Shan, in *Problems of Seismicity of the Far East,* p. 33, Nauka, Khabarovsk.

Garagash, I. A., L. I. Lobkovsky, O. R. Kozyrev, and R. Kh. Mazova (2003), Generation and run-up of tsunami waves due to submarine landslide, *Oceanology, 43*(2), 185.

Garagash, I. A., and L. I. Lobkovsky (2006), An analysis of the dynamic displacement process of the sea bottom due to a subduction zone earthquake, in *Proc. of 4th International FLAC Symposium on Numerical Modeling in Geomechanics,* p. 321, Balkema Press, Madrid.

Goto, C., Y. Ogava, N. Shuto, and N. Imamure (1997), *Numerical Method of Tsunami Simulation with the Leap-Frog Scheme (IUGG/IOC Time Project),* Manual and Guides, No. 35, 4 Parts, 126 pp., UNESCO, Paris.

Hirata, K., K. Satake, Y. Tanioka, T. Kuragano, Y. Hasegawa, Y. Hayashi, and N. Hamada (2006), The 2004 Indian Ocean tsunami: Tsunami source model from satellite altimetry, *Earth Planets Space, 58(3),* 195.

Kulikov, E., I. Medvedev, and S. Lappo (2005), Satellite recording of the Indian Ocean tsunami on 26 December, 2004, *Dokl. Ros. Akad. Nauk, 401A,* 444.

Lay, T., H. Kanamori, C. Ammon, M. Nettles, S. Ward, R. Asteer, S. Beck, S. Bilek, M. Brudzinski, R. Butler, H. Deshon, G. Ekstrom, K. Satake, and S. Sipkin (2005), The great Sumatra-Andaman earthquake of 26 December, 2004, *Science, 308,* 1127, doi:10.1126/science.1112250.

Lobkovsky, L. I. (1988), *Geodynamics of Spreading and Subduction Zones, and Two-Level Plate Tectonics,* 253 pp., Nauka, Moscow.

Lobkovsky, L. I., V. I. Kerchman, B. V. Baranov, and E. I. Pristavkina (1991), Analysis of seismotectonic processes in subduction zones from the standpoint of a keyboard model of great earthquakes, *Tectonophysics, 199,* 211, doi:10.1016/0040-1951(91)90173-P.

Lobkovsky, L. I., A. M. Nikishin, and V. E. Khain (2004), *Current Problems of Geotectonics and Geodynamics,* 611 pp., Scientific World Press, Moscow.

Lobkovsky, L., R. Mazova, I. Garagash, L. Kataeva, and N. Petrukhin (2005a), Analysis of the 26 December, 2004 Earthquake and Tsunami in the Indian Ocean on the Basis of the Subduction Keyboard Model, Geophys. Res. Abstr. of EGU General Assembly, Austria, Vienna, 24–30 April 2005, 7, 00949.

Lobkovsky, L. I., R. Kh. Mazova, and L. Yu. Kataeva (2005b), The Source Mechanism of Indian Ocean Tsunami of 26 December, 2004, Proc. of Int. Tsunami Symposium, p. 295, Chania, Crete Isl., Greece, 27–29 June, 2005.

Lobkovsky, L. I., R. Kh. Mazova, B. V. Baranov, and L. Yu. Kataeva (2006), Generation and propagation of tsunami in the Sea of Okhotsk (possible scenarios), *Dokl. Ross. Akad. Nauk* (in Russian), *410,* 528.

Mazova, R. Kh., and J. F. Ramirez (1999), Tsunami wave with an initial negative wave on the Chilean coast, *Nat. Hazards, 20,* 83, doi:10.1023/A:1008160113672.

Okada, Y. (1992), Internal deformation due to shear and tensile faults in a half-space, *Bull. Seismol. Soc. Am., 82,* 1018.

Sielecki, A., and M. Wurtele (1970), The numerical integration of the nonlinear shallow water equations with sloping boundaries, *J. Comput. Phys., 6,* 219, doi:10.1016/0021-9991(70)90022-7.

Soloviev, S. L., A. V. Nekrasov, V. G. Bukhteev, and R. V. Pyaskovsky (1977), Preliminary tsunamizonation of Kurile-Kamchatka coast on the basis of hydrodynamical computations, in *Theoretical and Experimental Research on the Tsunami Problem,* p. 131, Nauka, Moscow.

Titov, V., A. Rabinovich, H. Mofjeld, R. E. Tomson, and F. I. Gonzalez (2005), The global reach of the 26 December Sumatra tsunami, *Science, 309,* 2045, doi:10.1126/science.1114576.

I. A. Garagash, Institute of Physics of the Earth, Russian Academy of Sciences, 10 B. Gruzinskaya Str., Moscow, Russia

L. I. Lobkovsky, P. P. Shirshov Institute of Oceanology, 36 Nakhimovskiy pr., Russian Academy of Sciences, Moscow, Russia

R. Mazova, L. Kataeva, I. Nardin, Nizhny Novgorod State Technical University, Nizhny Novgorod, 603600 Russia (raissamazova@mail.nnov.ru)